

Magnetization Decay due to Vortex Phase Boundary Motion in BSCCO

M. Konczykowski^a, C. J. van der Beek^a, S. Colson^a, M. V. Indenbom^{a,b}, P. H. Kes^c, Y. Paltiel^d, E. Zeldov^d

^aLaboratoire des Solides Irradiés, Ecole Polytechnique, 91128 Palaiseau, France

^bInstitute of Solid State Physics, 142432 Chernogolovka, Moscow District, Russia

^cKamerlingh Onnes Laboratorium, Rijksuniversiteit Leiden, The Netherlands

^dDepartment of Condensed Matter Physics, Weizmann Institute of Science, Rehovot, Israel

We identify a new regime of decay of the irreversible magnetization in clean $\text{Bi}_2\text{Sr}_2\text{CaCu}_2\text{O}_8$ crystals, at induction values close to the “second peak field” at which the bulk critical current density steeply increases. A time window is identified during which the decay of the induction is controlled by the slow propagation of the phase transformation front across the sample.

The origin of the second magnetization peak (SMP) manifest in $\text{Bi}_2\text{Sr}_2\text{CaCu}_2\text{O}_8$ (BSCCO) crystals at low temperature is the object of major controversy. Recent investigations of the role of weak disorder have confirmed its close relationship with the first order phase transition (FOT) observed at higher temperatures. This has led to a generic phase diagram of vortex matter [1–4], in which the SMP is thought to correspond to a phase transition from an ordered Bragg-glass at low vortex density (low fields) to a disordered vortex solid (glass) at high fields. One of the key experiments in favor of a phase transition at the

SMP was local magnetization, measured by the Hall-array technique [2]. Such measurements show a sharp increase of the induction gradient $\partial B/\partial x$ at a well-defined value of the induction B_{sp} , corresponding to the value at which the transition takes place. Here, we show from time resolved measurements of the induction that there exists a time regime during which the slow motion of the phase transformation front determines the global magnetic relaxation.

The lightly oxygen overdoped BSCCO crystal used in this study, cut from a larger crystal, was checked for its uniformity by magneto-optical imaging of the flux penetration. Local induction profiles were measured on the crystal surface using a 2D electron gas Hall-probe array, composed of 11 sensors of area $10 \times 10 \mu\text{m}^2$, and spaced by $10 \mu\text{m}$. Increasing (decreasing) branches of hysteretic “local magnetization” loops at various waiting times were obtained by swiftly ramping the applied field H_a up (down) to its target value from a starting point lower (higher) by several times the full penetration field, after which the magnetic relaxation was recorded during 350 s. On the experimental time scale ($t > 5$ s), the SMP at $T \gtrsim 25$ K is marked by the emergence of Bean-like induction profiles from dome-shaped profiles related to screening by the surface barrier currents. Only at temperatures below 20 K can one observe the SMP as a crossover from one bulk pinning regime to another. Fig. 1 shows loops of

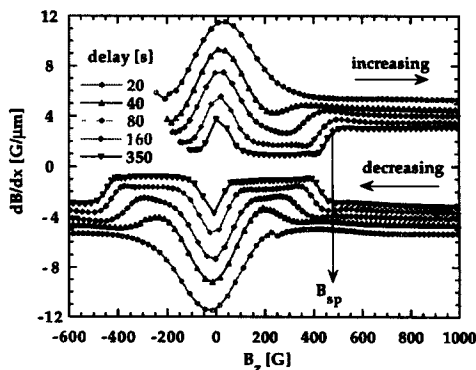


Figure 1. Hysteretic loops of the local induction gradient $\partial B/\partial x$ vs. B_z , recorded at 15.9 K, for various times after field application.

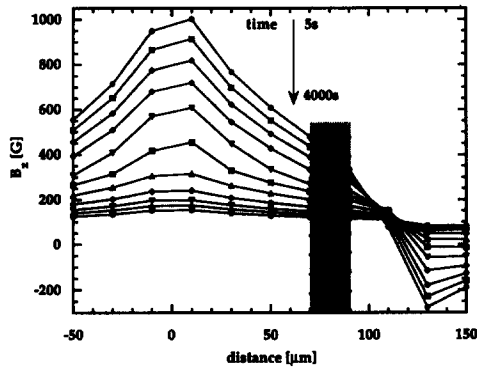


Figure 2. Decay of the magnetic induction on the surface of the BSCCO sample at $T = 15.9$ K and $H_a = 100$ Oe, after field-cooling in 3 kOe followed by the fast decrease of the applied field.

$\partial B/\partial x$ vs. the local induction B at various times after the end of the field ramp, for $T = 15.9$ K. The characteristic jump of $\partial B/\partial x$ at B_{sp} appears only at long times; at short times, *i.e.* at higher screening current, the inverse situation occurs and $\partial B/\partial x$ is higher for $B < B_{sp}$.

Long time relaxations at various applied fields H_a were recorded by cooling the sample down from $T > 30$ K in a field exceeding H_a by 3 kOe. After reaching thermal stability at 15.9 K, the field was rapidly decreased to H_a and the decay of the magnetic induction profiles was recorded during 4000 s (Fig. 2). From the spatially resolved magnetic relaxation, the electric field is obtained by summing the numerically calculated time derivatives $\partial B/\partial t$ for five sensors, from the center of the crystal outwards. Assuming that $\partial B/\partial x$ is proportional to the local current density j , and that the electric field arises as a result of thermally activated vortex creep Ref. [5], a plot of $U \propto kT \ln(E/B/j)$ against $\partial B/\partial x$ represents the variation of the flux creep energy barrier with current density (Fig. 3). When $H_a > B_{sp}$, ($H_a \geq 500$ Oe), smooth, power like variations $U \propto j^{-0.38}$ are obtained. A completely new behavior is observed when $H_a < B_{sp}$: then, the divergence of $U(j)$ stops at a given time, after which an extended plateau in the $U(j)$ curve appears. The correlation of the $U(j)$ -curves with the decaying flux profiles shows that the begin-

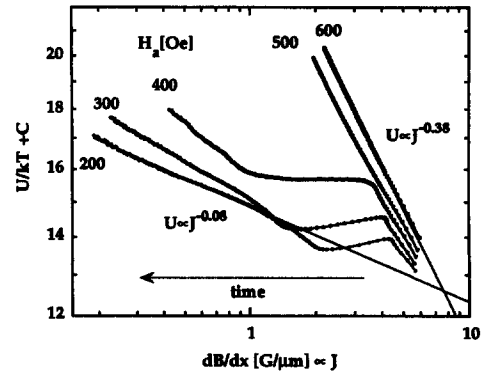


Figure 3. Flux creep activation barrier vs. current variations $U(j)$ in the BSCCO crystal at 15.9 K, for various applied fields.

ning of the plateau at high j corresponds to the first appearance of the low-field ordered vortex phase (identifiable in Fig. 2 by the smaller gradient $\partial B/\partial x$ in the crystal). The end of the plateau at long t or small j occurs when there is no region of high-field phase (corresponding to the region of higher $\partial B/\partial x$) left in the sample. Only then does a new power-law-like divergence of $U \sim j^{-0.08}$, representative of the activation barriers in the low-field phase, start. In the intermediate time interval, the relaxation process is determined by the slow motion of phase transformation front across the sample.

Concluding, the low-field and high-field vortex phases are characterized by very different $U(j)$ - (or $I(V)$ -) relations. The SMP occurs as a result of the jump from one $I(V)$ -curve to another. In the regime of phase coexistence at $B \sim B_{sp}$, the electrodynamic of the sample is determined by the motion of the phase transformation front.

REFERENCES

1. N. Chikumoto *et al.*, Phys. Rev. Lett. **69**, 1260 (1992)
2. B. Khaykovich *et al.*, Phys. Rev. Lett. **76**, 2555 (1996)
3. B. Khaykovich *et al.*, Phys. Rev. B **57**, R517 (1997)
4. V.M. Vinokur *et al.*, Physica C **295**, 209, (1998)
5. Y. Abulafia *et al.*, Phys. Rev. Lett. **77**, 1596 (1996).